A Novel Fast Algorithm Based on SMDWT for Visual Processing Applications

Chih-Hsien Hsia[1]
Dept. of E.E.
Tamkang University
Tamsui, Taipei, Taiwan
chhsia@ee.tku.edu.tw

Jing-Ming Guo[2]
Dept. of E.E.
National Taiwan University of Science and Technology
Taipei, Taiwan
jmguo@seed.net.tw

Jen-Shiun Chiang[1]
Dept. of E.E.
Tamkang University
Tamsui, Taipei, Taiwan
chiang@ee.tku.edu.tw

Chia-Hui Lin[1]
Dept. of E.E.
Tamkang University
Tamsui, Taipei, Taiwan
happy260000@hotmail.com

Abstract—**This work presents a fast algorithm, namely 2-D Symmetric Mask-based Discrete Wavelet Transform (SMDWT), to address some critical issues of the 2-D Discrete Wavelet Transform (DWT). Unlike the traditional DWT involving dependent decompositions, the SMDWT itself is subband processing independent, which can significantly reduce complexity. Moreover, DWT cannot directly obtain target subbands, which leads to an extra wasting in transpose memory, critical path, and operation time. These problems can be fully improved with the proposed SMDWT. Nowadays, many applications employ DWT as the core transformation approach, the problems indicated above have motivated researchers to develop fast algorithms for DWT. The proposed SMDWT has been proved as a highly efficient independent processing to yield target subbands which can be applied to real-time visual applications, such as moving object detection and tracking, texture segmentation, image/video compression, and any DWT-based applications.**

I. INTRODUCTION

Filter banks for the applications of subband visual coding were introduced in the 1990s. Wavelet coding has been studied extensively since then. Wavelet coding has been successfully applied to many applications. The most significant applications include subband coding for audio, image, video, signal analysis, and representation using wavelets. In the past few years, DWT [1] has been adopted in a wide range of applications including image coding and video compression, including speech analysis, numerical analysis, signal analysis, image coding, pattern recognition, computer vision and biometrics. The DWT can be viewed as a multi-resolution decomposition of a signal, meaning which decomposes a signal into several components in different wavelet frequency bands. By factoring the classical wavelet filter into lifting steps, the computational complexity of the corresponding DWT can be reduced by up to 50% [1]. The lifting steps can be easily implemented, which is different from the direct finite impulse response (FIR) implementations of Mallat's algorithm [1]. Moreover, wavelet-based is a modern tool for visual processing applications, such as JPEG2000 still image compression, computer vision, Motion-JPEG2000, Chinese writer identification, texture segmentation, denoising, watermarking , and face detection. Cheng *et al.* [5] used the DWT to detect and track moving objects. It only processes the part of LL band image due to the consideration of low computing cost and noise reduction issues. Lu *et al.* [6] proposed a mechanism for unsupervised texture segmentation. The proposed method utilizes a set of high frequency channel energies to characterize texture features, followed by a multithresholding technique for coarse segmentation. Although this method based on the traditional DWT, the four subband information produced by the window size via two dimensions (row and column) calculated may cause high computing cost in the processing. Çelik *et al.* [7] present a novel method for facial feature extraction using DWT to extract edge information using the six complex bands with different directionalities. A test statistics whose distribution matches very closely with the directional information in the six directional subbands of the DT-DWT is derived and used for detecting facial feature edges. However, the real-time 2-D DWT (software-based) is still difficult to be achieved. Hence, an efficient transformation scheme for large of multimedia files is highly demanded.

The rest of this paper is organized as follows. In Section II, the LDWT is briefly introduced. The proposed SMDWT approach is presented in Section III. Section IV demonstrates the performance comparisons. The conclusions are given in Section V.

II. LIFTING-BASED DISCRETE WAVELET TRANSFORM

The LDWT proposed by Daubechies and Sweldens requires fewer computations than the conventional convolution-based approach [1]. The lifting-based scheme is an efficient implementation of DWT [2]. The 2-D LDWT uses a vertical and horizontal 1-D LDWT subband decomposition to obtain the 2-D LDWT coefficients. And the coefficients of the Daubechies 9/7 decomposition filter are h[n] and g[n] as in [3]. The 9/7 filter has two lifting steps and one scaling step while the 5/3 filter [2] can be regarded as a special case with single lifting step. The detailed forward algorithm of the 9/7 filter is described from [3].

The lifting step associated with the wavelet is shown in Fig. 1. The original signals separate into s[n] and d[n] such as $s0$, $d0$, $s1$, $d1$, $s2$, $d2$, $s3$, $d3$, and $s4$. Assuming that the original data are infinite in length, the first stage lifting is first applied to update the odd index data $s0$, $s1$,…. In Eq. 1, the parameters

978-1-4244-3828-0/09/$25.00 ©2009 IEEE

α and d^1[n] represent the first stage lifting parameters and outcomes, respectively. After all the odd index data points are calculated, the second stage lifting could be performed with Eq. 2, where the parameters β and s^1[n] represent the second stage lifting parameters and outcomes, respectively. In Eqs. 3 and 4, the H[n] and L[n] are obtained from processing d^1[n] and s^1[n] by the parameters γ and δ, and for more accurate. Finally, through the normalization factors (1/ζ and ζ.) to obtain the high pass and low pass wavelet coefficients.

$$d^l[n] = d[n]+\alpha\times(s[n]+s[n+1]), \quad (1)$$
$$s^l[n] = s[n]+\beta\times(d[n-1]+d[n]), \quad (2)$$
$$H[n] = d^l[n]+\gamma\times(s^l[n]+s^l[n+1]), \quad (3)$$
$$L[n] = s^l[n]+\delta\times(d^l[n-1]+d^l[n]), \quad (4)$$
$$H[n] = [d^l[n]+\gamma\times(s^l[n]+s^l[n+1])]\times 1/\zeta, \quad (5)$$
$$L[n] = [s^l[n]+\delta\times(d^l[n-1]+d^l[n])]\times\zeta \quad (6)$$

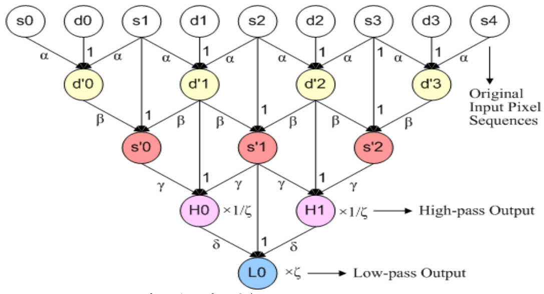

Fig. 1. The 9/7 LDWT structure.

III. THE PROPOSEDALGORITHM

The DWT is widely employed in the visual subband processing, since it inherently has the well-known perfect reconstruction property and it could analyze each subband for preprocessing. However, in 2-D transform, it has higher complexity, transpose memory, and critical path. Because the four subbands of the LDWT are all relation, we could not get the target subband immediately. It would waste the memory of unnecessary subbands operation time. In this work, the proposed 2-D 9/7 SMDWT could solve these problems by a single matrix (de-relation). It has many advantages such as low time complexity, simple and regular algorithm, and independent subbands for target application. The proposed method is introduced step by step in the following subsections, and the coefficients of mask wavelet coefficient the derivation is based on the 2-D 9/7 LDWT.

In speed and simplicity, generally, four masks, 7×7, 7×9, 9×7, and 9×9, are used to perform spatial filtering tasks. Moreover, the four-subband processing can be further optimized to speed up and reduce the computing cost of DWT coefficients. The four-matrix processors consist of four mask filters, and each filter is derived from one 2-D DWT of 9/7 float lifting-based coefficients. Since the transpose memory requirement of size N^2 (L and H frequency) is huge and the processing takes too much time, as shown in Fig. 2(a). In this work, a new approach, 2-D SMDWT, is introduced to reduce computing time and low complexity, as shown in Fig. 2(b). In Fig.2 as shown the data flow of the LDWT and the SMDWT. To achieve the 2-D LDWT might need a vertical and horizontal 1-D LDWT calculation, respectively. And each of 1-D LDWT would require calculating with four steps such as split, predict, update, and scaling. However, the four subbands of 2-D SMDWT are reached by a single matrix. And it only multiplies the coefficients of the mask during the procedure. Therefore, it presents results comparing with the LDWT, the SMDWT is more simple and regular.

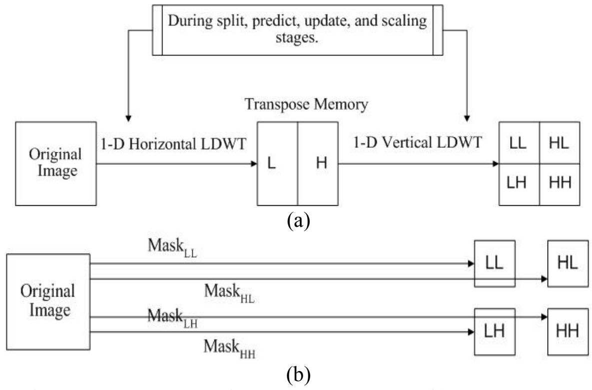

Fig. 2. Structure comparisons. (a) 2-D LDWT; (b) 2-D SMDWT.

First, we know the coefficients of LDWT are α=-1.586134342, β=-0.052980118, γ=0.882911075, δ=0.443506852, and ζ=1.230174105. And the Daubechies 9/7 filter needs nine original input pixels to produce one low pass wavelet coefficient as well as seven original input pixels to produce one high pass wavelet coefficient. Then, we would show how we obtain the four subbands mask-based (matrix) coefficients such as HH mask which is matrix of 7×7, LL mask which is matrix of 9×9, HL mask which is matrix of 9×7, and LH mask which is matrix of 7×9 in following:

A. *HH subband*

In this part, we would obtain a HH(x,y) which is the wavelet coefficient in HH band by decomposing the original pixel sequences form the original image.

The 2-D 9/7 LDWT uses a horizontal and vertical 1-D 9/7 LDWT subband decomposition to obtain the 2-D 9/7 LDWT coefficients. And then, we analyze the coefficients for obtaining the proposed 2-D 9/7 SMDWT coefficients.

Let A=s0, B=d0, C=s1, D=d1, E=s2, F=d2, and G=s3:

$d'0=\alpha A+B+\alpha C$, $d'1=\alpha C+D+\alpha E$, $d'2= \alpha E+F+\alpha G$,

$s'0=\beta\times(\alpha A+B+\alpha C)+C+\beta\times(\alpha C+D+\alpha E)$,

$s'1=\beta\times(\alpha C+D+\alpha E)+E+\beta\times(\alpha E+F+\alpha G)$,

$$H0=(1/\zeta)\times(\gamma\times(\beta\times(\alpha A+B+\alpha C)+C+\beta\times(\alpha C+D+\alpha E)))+(1/\zeta)\times(\alpha C\ D+\alpha E)+(1/\zeta)\times(\gamma\times(\beta\times(\alpha C+D+\alpha E)+E+\beta\times(\alpha E+F+\alpha G))) \quad (7)$$

This H0-point represent H(x-3,y) which is the high frequency wavelet coefficient. And then the vertical 1-D 9/7 LDWT subband decomposition structure:

Let A'=Hs0, B'=Hd0, C'=Hs1, D'=Hd1, E'=Hs2, F'=Hd2, and G'=Hs3: $Hd'0= \alpha A'+B'+\alpha C'$, $Hd'1= \alpha C'+D'+\alpha E'$, $Hd'2= \alpha E'+F'+\alpha G'$, $Hs'0= \beta\times(\alpha A'+B'+\alpha C')+C'+\beta\times(\alpha C'+D'+\alpha E')$, $Hs'1= \beta\times(\alpha C'+D'+\alpha E')+E'+\beta\times(\alpha E'+F'+\alpha G')$,

$$HH0=(1/\zeta)\times(\gamma\times(\beta\times(\alpha A'+B'+\alpha C')+C'+\beta\times(\alpha C'+D'+\alpha E')))+(1/\zeta)\times(\alpha C'+D'+\alpha E')+(1/\zeta)\times(\gamma\times(\beta\times(\alpha C'+D'+\alpha E')+E'+\beta\times(\alpha E'+F'+\alpha G'))) \quad (8)$$

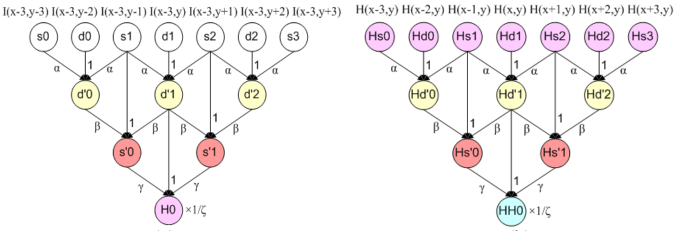

(a) (b)

Fig. 3. The 1-D 9/7 LDWT. (a) Horizontal direction; (b) Vertical direction.

This point represent HH(x,y) which is the high-high frequency wavelet coefficient. We get the HH(x,y) by 2-D 9/7 LDWT is now, next we will analyze H(x-3,y) and HH(x,y) coefficients of the equation for obtaining the 2-D 9/7 SMDWT HH subband mask coefficient. First, the H(x-3,y) can be derived as follows:

$$H(x-3,y)=(\alpha\beta\gamma/\zeta)\times A+(\beta\gamma/\zeta)\times B+(3\alpha\beta\gamma/\zeta)\times C+(\gamma/\zeta)\times C+(\alpha/\zeta)\times C+(2\beta\gamma/\zeta)\times D+(1/\zeta)\times D+(3\alpha\beta\gamma/\zeta)\times E+(\gamma/\zeta)\times E+(\alpha/\zeta)\times E+(\beta\gamma/\zeta)\times F+(\alpha\beta\gamma/\zeta)\times G \tag{9}$$

And then, we transform algebras A~G into the original pixel sequences (horizontal coefficients) I(x-3,y-3)~I(x-3,y+3). Transform algebras:

$$H(x-3,y)=(\alpha\beta\gamma/\zeta)\times I(x-3,y-3)+(\beta\gamma/\zeta)\times I(x-3,y-2)+(3\alpha\beta\gamma/\zeta)\times I(x-3,y-1)+(\gamma/\zeta)\times I(x-3,y-1)+(\alpha/\zeta)\times I(x-3,y-1)+(2\beta\gamma/\zeta)\times I(x-3,y)+(1/\zeta)\times I(x-3,y)+(3\alpha\beta\gamma/\zeta)\times I(x-3,y+1)+(\gamma/\zeta)\times I(x-3,y+1)+(\alpha/\zeta)\times I(x-3,y+1)+(\beta\gamma/\zeta)\times I(x-3,y+2)+(\alpha\beta\gamma/\zeta)\times I(x-3,y+3) \tag{10}$$

Moreover, let $Ha=\alpha\beta\gamma/\zeta$, $Hb=\beta\gamma/\zeta$, $Hc=\gamma/\zeta$, $Hd=\alpha/\zeta$, $He=1/\zeta$. The coefficient of H(x-3,y) could be calculated by:

$$H(x-3,y)=I(x-3,y-3)\times Ha+I(x-3,y-2)\times Hb+I(x-3,y-1)\times(3\times Ha+Hc+Hd)+I(x-3,y)\times(2\times Hb+He)+I(x-3,y+1)\times(3\times Ha+Hc+Hd)+I(x-3,y+2)\times Hb+I(x-3,y+3)\times Ha \tag{11}$$

Second, the HH(x,y) can be derived as follows:

$$HH(x,y)=(\alpha\beta\gamma/\zeta)\times A'+(\beta\gamma/\zeta)\times B'+(3\alpha\beta\gamma/\zeta)\times C'+(\gamma/\zeta)\times C'+(\alpha/\zeta)\times C'+(2\beta\gamma/\zeta)\times D'+(1/\zeta)\times D'+(3\alpha\beta\gamma/\zeta)\times E'+(\gamma/\zeta)\times E'+(\alpha/\zeta)\times E'+(\beta\gamma/\zeta)\times F'+(\alpha\beta\gamma/\zeta)\times G' \tag{12}$$

And then, we transform algebras A'~G' into the high frequency pixel sequences (vertical coefficients) H(x-3,y)~H(x+3,y). Transform algebras:

$$HH(x,y)=(\alpha\beta\gamma/\zeta)\times H(x-3,y)+(\beta\gamma/\zeta)\times H(x-2,y)+(3\alpha\beta\gamma/\zeta)\times H(x-1,y)+(\gamma/\zeta)\times H(x-1,y)+(\alpha/\zeta)\times H(x-1,y)+(2\beta\gamma/\zeta)\times H(x,y)+(1/\zeta)\times H(x,y)+(3\alpha\beta\gamma/\zeta)\times H(x+1,y)+(\gamma/\zeta)\times H(x+1,y)+(\alpha/\zeta)\times H(x+1,y)+(\beta\gamma/\zeta)\times H(x+2,y)+(\alpha\beta\gamma/\zeta)\times H(x+3,y) \tag{13}$$

Moreover, let $Ha=\alpha\beta\gamma/\zeta$, $Hb=\beta\gamma/\zeta$, $Hc=\gamma/\zeta$, $Hd=\alpha/\zeta$, $He=1/\zeta$. Since, the HH(x,y) general form can be expressed as:

$$HH(x,y)=H(x-3,y)\times Ha+H(x-2,y)\times Hb+H(x-1,y)\times(3\times Ha+Hc+Hd)+H(x,y)\times(2\times Hb+He)+H(x+1,y)\times(3\times Ha+Hc+Hd)+H(x+2,y)\times Hb+H(x+3,y)\times Ha \tag{14}$$

Third, we order the HH(x,y) corresponding coefficients relate to the original sequences. The HH(x,y) can be derive a 7×7 matrix which represents the original sequences would multiplied by from the above H(x-3,y) and HH(x,y). And the matrix is just the 2-D 9/7 SMDWT HH subband mask what we want.

First, the 7×7 matrix which is the input pixel multiplied by the corresponding coefficients of each H(x-3,y)~H(x+3,y). Next, we take the 7×7 matrix which is the input pixel multiplied extra by the corresponding coefficients of HH(x,y) equations which is towards each H(x-3,y)~H(x+3,y).

Next, we can be derive the 7×7 matrix which is the input pixel should totally multiply to obtain the HH(x,y) instantly.

Finally, we can be derive a 2-D 9/7 SMDWT 7×7 matrix of HH subband which can immediately obtain the HH coefficient form 2-D 9/7 LDWT. The coefficients of mask are as below:

Let $HH\alpha=Ha\times Ha$, $HH\beta=Ha\times Hb$, $HH\gamma=Ha\times(3\times Ha+Hc+Hd)$, $HH\delta=Ha\times(2\times Hb+He)$, $HH\varepsilon=Hb\times Hb$, $HH\eta=Hb\times(2\times Hb+He)$, $HH\theta=(3\times Ha+Hc+Hd)\times(3\times Ha+Hc+Hd)$, $HH\zeta=Hb\times(3\times Ha+Hc+Hd)$, $HH\iota=(3\times Ha+Hc+Hd)\times(2\times Hb+He)$, $HH\kappa=(2\times Hb+He)\times(2\times Hb+He)$

$$\begin{aligned}HH_{7\times7}(x,y)=&HH_{\alpha}\times\{\sum_{i=0}^{1}\sum_{j=0}^{1}I(2x-3+6i,2y-3+6j)\}+HH_{\beta}\times\{\sum_{i=0}^{1}\sum_{j=0}^{1}[I(2x-2+4i,2y-3+6j)+I(2x-3+6i,2y-2+4j)]\}\\&+HH_{\gamma}\times\{\sum_{i=0}^{1}\sum_{j=0}^{1}[I(2x-1+2i,2y-3+6j)+I(2x-3+6i,2y-1+2j)]\}+HH_{\delta}\times\{\sum_{j=0}^{1}I(2x,2y-3+6j)+\sum_{i=0}^{1}I(2x-3+6i,2y)\}\\&+HH_{\varepsilon}\times\{\sum_{i=0}^{1}\sum_{j=0}^{1}I(2x-2+4i,2y-2+4j)\}+HH_{\zeta}\times\{\sum_{i=0}^{1}\sum_{j=0}^{1}[I(2x-1+2i,2y-2+4j)+I(2x-2+4i,2y-1+2j)]\}\\&+HH_{\eta}\times\{\sum_{j=0}^{1}I(2x,2y-2+4j)+\sum_{i=0}^{1}I(2x-2+4i,2y)\}+HH_{\theta}\times\{\sum_{i=0}^{1}\sum_{j=0}^{1}I(2x-1+2i,2y-1+2j)\}\\&+HH_{\iota}\times\{\sum_{j=0}^{1}I(2x,2y-1+2j)+\sum_{i=0}^{1}I(2x-1+2i,2y)\}+HH_{\kappa}\times I(2x,2y)\end{aligned} \tag{15}$$

B. LL, HL, and LH subband

The LL, HL, and LH band could be derived in the same way. According to the 2-D 9/7 LDWT, the LL, HL, and LH band coefficients of the SMDWT could be expressed as follows, respectively. (Because limit page, so we present important band equations in this paper)

$$\begin{aligned}LL_{9\times9}(x,y)=&LL_{\alpha}\times\{\sum_{i=0}^{1}\sum_{j=0}^{1}I(2x-4+8i,2y-4+8j)\}+LL_{\beta}\times\{\sum_{i=0}^{1}\sum_{j=0}^{1}[I(2x-3+6i,2y-4+8j)+I(2x-4+8i,2y-3+6j)]\}\\&+LL_{\gamma}\times\{\sum_{i=0}^{1}\sum_{j=0}^{1}[I(2x-2+4i,2y-4+8j)+I(2x-4+8i,2y-2+4j)]\}+LL_{\delta}\times\{\sum_{i=0}^{1}\sum_{j=0}^{1}[I(2x-1+2i,2y-4+8j)+I(2x-4+8i,2y-1+2j)]\}\\&+LL_{\varepsilon}\times\{\sum_{j=0}^{1}I(2x,2y-4+8j)+\sum_{j=0}^{1}I(2x-4+8i,2y)\}+LL_{\zeta}\times\{\sum_{i=0}^{1}\sum_{j=0}^{1}I(2x-3+6i,2y-3+6j)\}\\&+LL_{\eta}\times\{\sum_{i=0}^{1}\sum_{j=0}^{1}[I(2x-2+4i,2y-3+6j)+I(2x-3+6i,2y-2+4j)]\}+LL_{\theta}\times\{\sum_{i=0}^{1}\sum_{j=0}^{1}[I(2x-1+2i,2y-3+6j)+I(2x-3+6i,2y-1+2j)]\}\\&+LL_{\iota}\times\{\sum_{j=0}^{1}I(2x,2y-3+6j)+\sum_{j=0}^{1}I(2x-3+6i,2y)\}+LL_{\kappa}\times\{\sum_{i=0}^{1}\sum_{j=0}^{1}I(2x-2+4i,2y-2+4j)\}\\&+LL_{\lambda}\times\{\sum_{i=0}^{1}\sum_{j=0}^{1}[I(2x-1+2i,2y-2+4j)+I(2x-2+4i,2y-1+2j)]\}+LL_{\mu}\times\{\sum_{j=0}^{1}I(2x,\end{aligned}$$

$$2y-2+4j)+\sum_{j=0}^{1} I(2x-2+4i,2y)\}+LL_{v}\times\{\sum_{i=0}^{1}\sum_{j=0}^{1} I(2x-1+$$
$$2i,2y-1+2j)\}+LL_{\xi}\times\{\sum_{j=0}^{1} I(2x,2y-1+2j)+\sum_{j=0}^{1} I(2x-1+$$
$$2i,2y)\}+LL_{o}\times I(2x,2y) \qquad (16)$$

IV. EXPERIMENTAL RESULTS

In this section, the performance of the 2-D 9/7 SMDWT is evaluated in terms of its complexity and practical execution time. The discussion above shows that the complexity of the proposed SMDWT can be significantly reduced by exploiting the symmetric feature of the masks, and the four-matrix frameworks, HH, HL, LH, and LL lead to four subband different applications. Table 1 shows the analysis results of the complexity between the conventional 2-D Lifting DWT [3] and the 2-D SMDWT scheme for obtaining the LL band images. Herein, the Big-*O* denotes the computation complexity. It is clear that the ratio between LDWT [3] and SMDWT at all levels are equivalent to 4.2%; the ratio.

And then, In [3], it transforms an image into four-subband images with the Lifting coefficients DWT [3]. The overall computational complexity can be evaluated as below:

$$\mathrm{C}=\sum_{L=1}^{L}\left(\frac{N^2}{2^{2L-1}}\times 6+\frac{N^2}{2^{2L}}\times 12\right) \qquad (17)$$

On the other hand, the SMDWT directly transforms an original image into four-subband images using the four derived masks which does not need to process row and column data separately. In addition, it simply calculates even pixels for every row and column during the transforming process. The overall computational complexity of the SMDWT is represented as below.

$$\mathrm{C}=\sum_{i=1}^{L}\frac{N^2}{4^L} \qquad (18)$$

V. CONCLUSIONS

This work proposes the 2-D SMDWT fast algorithm. The algorithm solves the computing complexity problem in the previous schemes caused by multiple-layer transpose decomposition operation. Hence, it is superior to the former 2-D DWT or 2-D LDWT approaches. According to practical execution time evaluation, the proposed method is around seven times faster than LDWT.

Since the proposed 2-D SMDWT algorithm has the advantages of a fast computational speed, and regular data flow. It is suitable for real-time visual processing or any DWT-based technology applications. Possible future works are described below:

1) Moving object detection and tracking using the LL-Mask of SMDWT: Video tracking systems have to deal with variously shape and size input objects, which often results in a poor computing cost. Cheng *et al.* [5] used the Daubehies DWT to detect and track moving objects. The 2-D DWT can be used to decompose an image into four-subband images (LL, LH, HL, and HH). It only processes the part of LL band image due to the consideration of low computing cost and noise reduction issues. Although this method provides low computing cost for post-processing and noise reduction based on the traditional DWT, the LL band image produced by the original image size via two dimensions (row and column) calculated may cause high computing cost in the pre-processing. In particular, they use the three-level DWT that not only raising great image transform computation, but also incurring slow motion of the moving objects.

2) Facial feature extraction using HL- or LH-Mask of SMDWT: Çelik *et al.* [7] presented a novel method for facial feature extraction using DWT. The model is developed with a unimodal Gaussian distribution using the skin region to detect edge map obtained from the DWT. Facial feature extraction is then performed by combining the edge information obtained by using DWT and the non-skin skin areas obtained from the pixel statistics. The above-mentioned procedure can be substituted using the proposed HL- or LH-Mask processing of SMDWT.

3) Texture segmentation using HH-Mask of SMDWT: Lu *et al.* [6] proposed a mechanism for unsupervised texture segmentation. The proposed method utilizes a set of high frequency channel energies to characterize texture features, followed by a multithresholding technique for coarse segmentation. The coarsely segmented results at the same scale are incorporated by an intra-scale fusion procedure. A fine segmentation technique is then used to reclassify the ambiguously labeled pixels generated from the intra-scale fusion step. Since the proposed HH-Mask processing SMDWT can be executed independently, it can be exploited in this application to significantly improve the performance.

REFERENCES

[1] I. Daubechies and W. Sweldens, “Factoring wavelet transforms into lifting steps,” *The Journal of Fourier Analysis and Applications*, vol. 4, no.3, pp. 247-269, 1998.

[2] J.-S. Chiang, C.-H. Hsia, H.-J. Chen, and T.-J. Lo, “VLSI architecture of low memory and high speed 2-D lifting-based discrete wavelet transform for JPEG2000 applications,” *IEEE International Symposium on Circuits and Systems,* pp. 4554-4557, May 2005.

[3] *JPEG2000 Part 1 Final Committee Draft Version 1.0, ISO/IEC JTC1/SC29 WG1*, Information Technology, April 2000.

[4] ISO/IEC JTC1/SC29/WG1 Wgln 1684, JPEG 2000 Verification Model 9.0, 2000.

[5] F.-H. Cheng and Y.-L. Chen, “Real time multiple objects tracking and identification based on discrete wavelet transform,” *Pattern Recognition*, vol. 39, no. 3, pp. 1126-1139, June 2006.

[6] C.-S. Lu, P.-C. Chung, and C.-F. Chen, “Unsupervised texture segmentation via wavelet transform,” *Pattern Recognition*, vol. 30, no. 5, pp.729-742, May 1997.

[7] T. Çelik, H. Özkaramanlı, and H. Demirel, “Facial feature extraction using complex dual-tree wavelet transform,” *Pattern Recognition*, vol. 111, no. 2, pp.229-264, January 2008.